

# Discharge rate measurements for Micromegas detectors in presence of a longitudinal magnetic field

B. Moreno<sup>\*,a</sup>, S. Aune<sup>b</sup>, J. Ball<sup>a</sup>, G. Charles<sup>a</sup>, A. Giganon<sup>b</sup>, P. Konczykowski<sup>a</sup>,  
C. Lahonde-Hamdoun<sup>b</sup>, H. Moutarde<sup>a</sup>, S. Procureur<sup>a</sup>, F. Sabatié<sup>a</sup>

<sup>a</sup>CEA, Centre de Saclay, Irfu/SPhN, 91191 Gif sur Yvette, France.

<sup>b</sup>CEA, Centre de Saclay, Irfu/Sedi, 91191 Gif sur Yvette, France.

---

## Abstract

We present discharge rate measurements for two Micromegas detectors using a photon beam impinging a CH<sub>2</sub> target in the Hall B of the Jefferson Laboratory. One detector was equipped with an additional GEM foil, and a reduction of the discharge probability by two orders of magnitude compared to the stand-alone Micromegas was observed. The detectors were placed in the FROST solenoid providing a longitudinal magnetic field up to 5 T. It allowed for precise measurements of the discharge probability dependence with a diffusion reducing magnetic field, for a possible use of Micromegas in the Forward Vertex Tracker (FVT) of the future CLAS12 spectrometer. Between 0 and 5 T, the discharge probability increased by a factor of 10 for polar angles between 19° and 34°, thus requiring the use of additional GEM foils to withstand the standard CLAS12 luminosity.

*Key words:* Micro Pattern Gaseous Detectors, Micromegas, GEM, Discharge, Spark, Magnetic field, CLAS, CLAS12, JLab.

*PACS:* 29.40.Cs, 29.40.Gx

---

## 1. Introduction

### 1.1. Motivation

Since its beginning in the 60s, the experimental study of the nucleon structure has triggered more and more efforts in designing detection systems and in increasing the luminosity of the successive machines. Theoretical tools have been developed that offer the most complete view of the nucleon, allowing for its tomography through a precise mapping of Generalized Parton Distribution functions (GPDs) [1]. The study of these GPDs require *exclusive* measurements, where all particles of a given reaction are detected, as well as high luminosity to compensate for very small cross sections. The future CLAS12 spectrometer [2] in the Hall B of the Jefferson Laboratory (USA) will fulfill these two requirements by using the upgrade of the accelerator from 6 to 12 GeV electrons as well as a new tracking system that will cover a large angular acceptance from 5 to 125 degrees. This tracker will include a completely new vertex detector for which

---

<sup>\*</sup>Email address: brahim.moreno@cea.fr.

Micromegas [3] have been proposed both in the recoil (Barrel) and Forward part. In the latter case, three double layers of flat disks Micromegas will operate with several MHz of background and in the presence of a 5 T longitudinal magnetic field. Such a specific environment may potentially lead to discharges (or sparks) occurring between the micro-mesh and the readout strips. High discharge rates can reduce the detector efficiency and degrade the tracking performance. In particular, a diffusion reducing magnetic field is likely to affect the discharge probability by increasing the local charge density in the detector. Preliminary studies with an  $^{241}\text{Am}$  source placed in a 1.5 T magnetic field suggested a strong effect on the sparking probability.

### 1.2. Goals of the tests

The main goal of these tests was therefore to measure the dependence of the sparking probability with a longitudinal magnetic field, and estimate the total spark rate for the Micromegas of the FVT in their CLAS12 environment. The detector prototypes were designed to allow for spark measurements at different polar angles with respect to the beam axis. Anticipating a large increase of the sparking probability with the magnetic field, these tests also aimed at investigating a possible reduction of this probability by using a modified detector.

## 2. Experiment

### 2.1. Prototypes

Special prototypes had to be built for these tests, in particular to fit inside the 5 T solenoid (visible at the center of Fig. 1, right). The PCB consisted of a 110 mm diameter disk as shown in Fig. 1 (left), with a 14 mm central hole for the beam. Detectors were divided into three regions defined by the three annular anodes engraved on the PCB. The micro-mesh of each detector was common to all three regions. The anodes could be separately grounded from the bottom side to measure the spark rate for different polar angles. Starting from the region closest to the beam, anodes are in the following referred to as the inner, central and outer anode, respectively. The polar angle coverage of the electrodes is given in Table 1. It is close to the anticipated CLAS12 FVT acceptance,  $\theta \in [5^\circ, 35^\circ]$ .

Anode	Polar angle coverage [deg]
Inner	$7.9 \leq \theta \leq 18.3$
Central	$18.7 \leq \theta \leq 27.3$
Outer	$27.6 \leq \theta \leq 33.5$

Table 1: Anodes polar angle coverage.

Both detectors were built at the Saclay MPGD<sup>1</sup> workshop with a 128  $\mu\text{m}$  amplification gap between the anodes and the stainless steel micro-mesh by using the *bulk* technology [4]. A 100  $\mu\text{m}$  aluminized Mylar foil was used as the drift electrode with a 5 mm conversion gap ensured by a Plexiglass frame. For the second detector, a 50  $\mu\text{m}$  GEM foil made at CERN was glued on a separate frame and mounted 2.3 mm above the micro-mesh.

Prior to the installation in the Hall B, gain measurements for the standard detector were performed with the same gas as for the tests (90% Ar-10%  $\text{iC}_4\text{H}_{10}$  in volume) using a  $^{55}\text{Fe}$  source.

<sup>1</sup>Stands for Micro Pattern Gaseous Detector

For practical reasons the Micromegas-GEM (referred to as MM-GEM in the following) was not calibrated before the beam tests. As the GEM of this detector went into short-circuit during the experiment, no absolute calibration could be performed. However, it was observed for the Micromegas (MM) that the current induced by the beam on the micro-mesh as a function of its high voltage varied similarly to the gain, as illustrated in Fig. 2. This observation was used for the Micromegas-GEM to calibrate its gain, the current having been monitored during the tests. After the GEM foil short-circuited, it was used as the drift electrode for this prototype leading to a Micromegas with a 2.3 mm drift gap.

## 2.2. Experimental setup

The tests took place in the Hall B of the Jefferson Laboratory in August 2010. We made use of the FROST experimental setup <sup>2</sup>, and in particular the 5 T solenoid magnet shown in Fig. 1 (right). The photon beam was obtained from the interaction of a 5.57 GeV electron beam on a Pt radiator of a few micron thickness ( $9 \times 10^{-3} X_0$ ). The scattered electrons were then bended and detected in a tagger system for luminosity monitoring. Only photons between 1.11 and 5.29 GeV in the whole Bremsstrahlung spectrum were actually tagged, and simulations showed that they represent around 16% of all the photons interacting with the target. The beam current was varied between 1 and 30 nA, leading to fluxes up to  $4 \times 10^8$  photons per second in the tagger energy range. During our tests, the FROST cryogenic target was emptied, and replaced by a 19.3 mm thick  $\text{CH}_2$  target, whose center was located 65 mm upstream of the detector. Both were fixed together inside the solenoid with a plastic cylinder. We started our measurements with the standard Micromegas (1.5 day), then removed it to install the one equipped with the GEM foil (1 day). In total, 34 hours of data taking were recorded, corresponding to approximately 24,000 sparks.

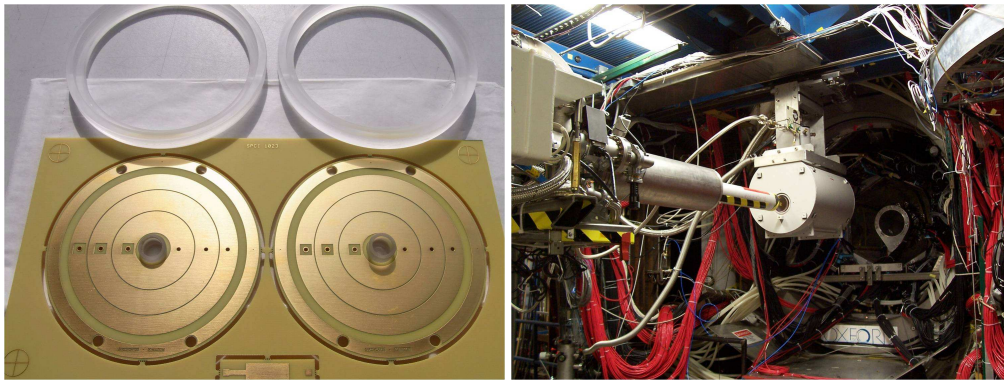


Figure 1: Detectors and experimental setup. On the left-hand side a picture of the PCB layouts designed for the two detectors. A photograph of the experimental setup with the beam line and the FROST solenoid at the center is displayed on the right-hand side.

## 2.3. Spark monitoring

Sparks were monitored by measuring the variation of the micro-mesh potential through a capacitor [5], a spark inducing a rapid increase of the micro-mesh current. The signal after being

<sup>2</sup>A description of it may be found in the experiment proposal [6].

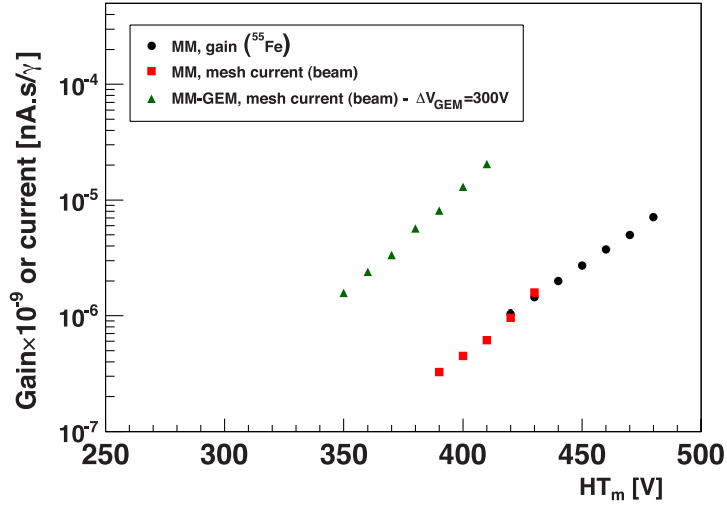


Figure 2: Gain measurements with a  $^{55}\text{Fe}$  source and mesh currents monitored during the tests for the 2 detectors. The comparison of the two measurements allows for the gain determination for the detector with the GEM foil.

amplified was fed to a discriminator, whose threshold had been tuned to tag every spark. A scaler was used to record the number of sparks for each run. The electron beam position and intensity were also recorded to correct the sparking probability for intensity variations and reject running periods with beam instabilities.

### 3. Results

Several measurements of the sparking probability were performed for both the Micromegas and the MM-GEM. Micro-mesh current instabilities occurred for the Micromegas with the inner anode grounded at the nominal gain,  $G = 1000$ , whether the beam was on or not. Therefore this electrode was not used and only the central and outer anodes were grounded for the measurements associated with this detector.

The sparking probability per incident particle on the target was the observable extracted. This physical quantity was calculated by dividing for each run the number of sparks by the averaged photon flux on the target in the tagger energy range. Running periods with beam position instabilities were discarded to avoid systematic effects.

The gain dependency is dealt with first. A presentation and a discussion of the effects of a longitudinal magnetic field follow.

#### 3.1. Effect of the gain on the sparking probability

The measurements of the sparking probability are presented in Fig. 3 as a function of the gain. These results were obtained at 0 T. The sparking probability goes approximately from  $P = 5.9 \times 10^{-11}$  to  $P = 2.9 \times 10^{-9}$  for the Micromegas over the gain range [400, 1446]. Concerning the MM-GEM its probability of sparking ranges from  $P \approx 1.6 \times 10^{-12}$  to  $P \approx 4.5 \times 10^{-9}$  for gains of  $G \approx 1000$  and  $G \approx 8474$ , respectively. The sparking probability exhibits a power law dependency with a similar slope for both detectors over most of the gain range. The only

deviation observed is for the MM-GEM at a gain of  $G \approx 10^3$  with a drop of about one order of magnitude compared to the value obtained by extrapolating the measurements at higher gains to  $G = 10^3$ . The addition of a GEM foil decreases the sparking probability by almost two orders of magnitude with respect to the Micromegas at a given gain.

Dedicated studies of MM-GEM [7] showed that at moderate GEM gain discharges for this type of detector mainly originate from energy deposit in the transfer gap, *i.e.* between the GEM foil and the micro-mesh. At a given detector gain the splitting of the MM-GEM gain between the GEM foil and the Micromegas reduces the sparking probability of the Micromegas by decreasing its gain. By further increasing the GEM gain, discharges mainly come from energy deposits in the drift gap. However the transverse diffusion for primary electrons produced in the drift gap reduces the charge density and therefore the sparking probability remains lower than that of a stand-alone Micromegas.

The observed behaviours are similar to what was obtained in previous tests with a hadron beam of 150 GeV [8].

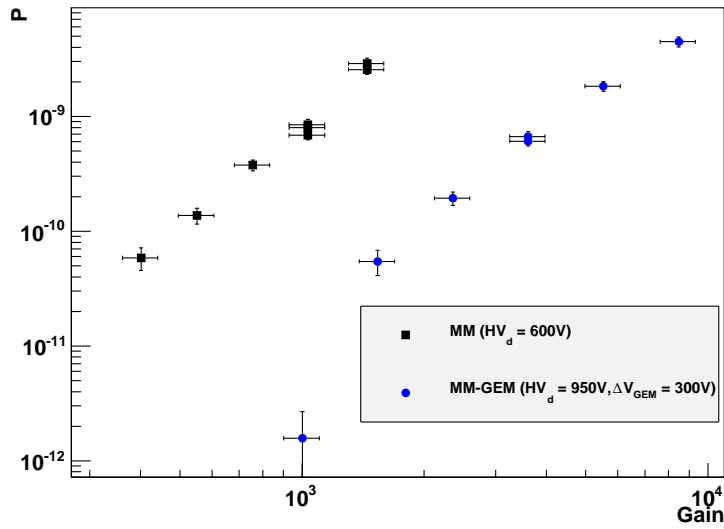


Figure 3: Sparking rate per particle on the target for the Micromegas and the MM-GEM. The results are plotted as a function of the detectors gain. The full squares (full circles) correspond to the Micromegas (MM-GEM). The drift field  $HV_d$  for the Micromegas and the MM-GEM were set to 600 V and 950 V respectively corresponding to a drift field. The high voltage difference between the two electrodes of the GEM foil was  $\Delta V_{GEM} = 300$  V.

### 3.2. Effect of a longitudinal magnetic field

A precise study of the effect of a longitudinal magnetic field on the sparking probability was performed for the Micromegas. The results are shown on the left-hand side of Fig 4. Between  $B = 0$  T and  $B = 1$  T, the sparking probability  $P$  is constant within error bars,  $P \approx 6.5 \times 10^{-10}$ . It increases up to  $P \approx 6 \times 10^{-9}$  at  $B = 4.4$  T and then remains stable. The sparking probability is multiplied by a factor 10 between  $B = 0$  T and  $B = 5$  T. This observation is independent of the gain as illustrated in Fig. 4 (right). The observed increase of the sparking probability is a

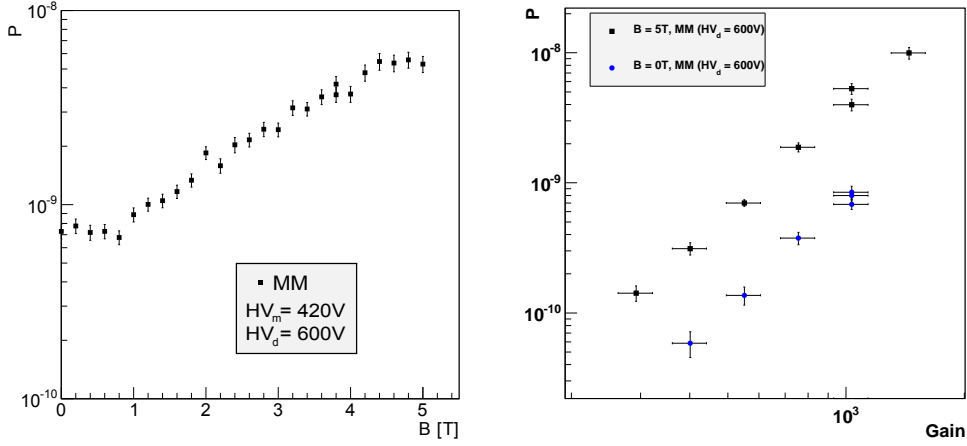


Figure 4: Sparking rate per particle on the target for the Micromegas detector in the presence of a longitudinal magnetic field. On the left-hand side, results are plotted as a function of the magnetic field amplitude for a detector gain of  $G \approx 1000$  and a drift field of 360 V/cm. On the right-hand side the sparking probability is shown as a function of the gain at  $B = 0$  T (full circles) and  $B = 5$  T (full squares) for a drift electrode high voltage of  $HV_d = 600$  V.

consequence of the concentrating effect of the longitudinal magnetic field. As the magnetic field strength augments, the diffusion of the primary electrons is more limited. It leads to a higher electron density and thus a higher sparking probability.

The polar angle dependency of the sparking probability in the presence of a longitudinal magnetic field was also investigated. Results are shown in Fig. 5 for the MM-GEM with the GEM foil acting as the drift electrode<sup>3</sup>. Over most of the measurement range the sparking probabilities for the central (full circles) and outer (up triangles) electrodes behave the same and are equal within error bars. As expected, the variation of the sparking probability with the central and outer anodes grounded (down triangles) is similar to that of the Micromegas in the same experimental conditions. There is an increase by a factor of 10 of the sparking probability between 0 and 5 T.

The region closest to the beam corresponding to the inner electrode (full squares) has the highest sparking probability in the whole magnetic field range, almost one order of magnitude larger than others one-electrode configurations. The probability of sparking decreases from  $P \approx 1.2 \times 10^{-8}$  to  $7.9 \times 10^{-9}$  before it starts going up at  $B = 2$  T. It finally reaches  $1.6 \times 10^{-8}$  at  $B = 5$  T. An explanation of this observed behaviour may be the following. With the magnet off, none of the charged particles produced by interaction of the beam with the target are diverted leading to high particle flux on the detector which produces charge pile-up. Such an effect is likely to produce a large number of primary electrons which once multiplied in the amplification gap may produce a sufficiently high electron density for the detector to spark. By augmenting the magnetic field, this effect is reduced as more and more particles trajectories are bent and fit in the detector beam hole. However, this effect is counter-balanced by the concentrating power of the increasing magnetic field on drift electrons, as explained previously.

Concerning the overall sparking probabilities with all electrodes grounded, it appeared com-

<sup>3</sup>The two GEM foil electrodes were put to the same high voltage.

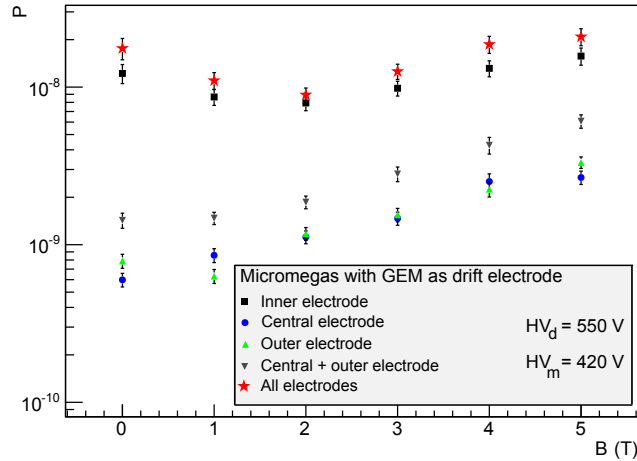


Figure 5: Effect of the polar angle on the sparking probability in the presence of a longitudinal magnetic field. The sparking probabilities are shown for the MM-GEM detector with the GEM foil acting as the drift electrode and plotted as a function of the magnetic field amplitude for a detector gain of  $G \approx 1000$  and a drift field of 565 V/cm. The drift electrode high voltage was set to  $HV_d = 550$  V.

pletely driven by the region closest to the beam.

#### 4. Comparison of the sparking probability with Geant4 simulation

A Geant4 simulation of the experimental setup has been performed, in order to reproduce the measured spark probability through the study of large energy deposits [9]. As ten electrons are needed on average to create one photon through the radiator, the following procedure was used to reduce the simulation time by an order of magnitude:

- in a first step, only the electron beam and the radiator were simulated, to extract the photon energy distribution;
- this energy distribution was then used to directly generate the photons.

It turns out that the tagger monitors only a small fraction ( $\approx 16\%$ ) of the photons, as illustrated in Fig. 6 (left). In Fig. 6 (right) are therefore compared the measured and simulated spark probabilities scaled to the total photon flux. With a Raether limit  $R_L$  of  $2.5 \times 10^7$  electrons, no significant differences are observed between experimental and simulated data for magnetic fields between 0 and 5 T. A similar simulation has been performed using a longitudinal magnetic field. No significant differences have been observed on the spark probability between 0 and 5 T. This confirms that the measured variation with the magnetic field can only come from a focusing of the electrons in the detector, leading to an increase of the local charge density. If the Raether limit could be usually expressed in terms of a maximum number of electrons in standard configurations, this measurement proves that the relevant parameter is rather the local charge density.

As the simulation gave a correct estimate of the spark probability for this particular setup (and at 0 T), it has been used to predict the spark rate in the final CLAS12 configuration. This

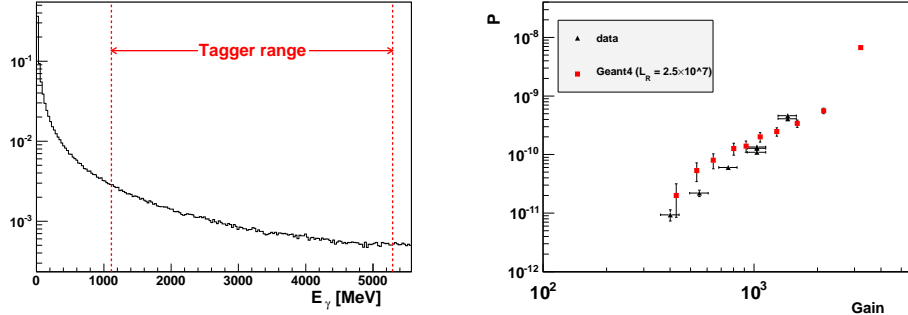


Figure 6: (Left): energy distribution of photons converted in the radiator, compared to the tagger energy range; (right): spark probability per incident photon on the target for experimental (full triangles) and simulated (full squares) data for the two outer anodes of the Micromegas detector.

includes the use of a Neon-based gas mixture in order to further decrease the discharge probability. Assuming that the effects of the magnetic field and of the GEM foil are similar in Neon gas, an overall sparking rate of a few Hz has been found per detector. Using a reasonable segmentation of the detectors micro-mesh, rates lower than 1 Hz could be achieved per independent micro-mesh.

## 5. Conclusion

First sparking probabilities measurements in the presence of a high longitudinal magnetic field were presented. They were performed in the context of the upgrade of the CLAS spectrometer, more precisely for the Forward Vertex Tracker of CLAS12. The main experimental conclusions of these tests are the following. For the polar angle region defined as  $19^\circ \leq \theta \leq 34^\circ$ , the sparking probability increases by a factor of 10 between  $B = 0$  T and  $B = 5$  T. Therefore the use of an additional GEM foil seems to be promising with a one-order-of-magnitude reduction of the sparking probability at  $B = 0$  T with respect to that of a Micromegas in the same conditions. However further measurements are needed to confirm this observation at  $B \neq 0$  T. To do so an experiment is being carried out with a 1.5 T magnet at the CEA Saclay with a  $^{241}\text{Am}$  radioactive source. The polar angle region between  $8^\circ \leq \theta \leq 18^\circ$  sparks ten times more than larger angle regions. One way of reducing the subsequent dead time would be to segment the micro-mesh so that when a spark occurs in the inner region the outer one is not blinded too. Studies are currently undergoing at the Saclay MPGD workshop with this in mind. By using the simulation calibrated on the data presented here, a sparking rate of the order of 1 Hz per detector is predicted in the final CLAS12 configuration for a Neon-based gas mixture.

## Acknowledgments

We would like to thank all the Hall B staff for their help during these tests, and particularly V. Burkert for the dedicated beam time, and S. Cristo for the installation of the detectors in CLAS. We are also grateful to M. Anfreville and his staff who built the two bulk detectors.

## References

- [1] A.V. Belitsky, A.V. Radyushkin, Phys.Rept. **418** (2005) 1-387.
- [2] CLAS12 web page, <http://www.jlab.org/Hall-B/clas12/>.
- [3] Y. Giomataris *et al.*, Nucl. Instrum. Methods A **376** (1996) 29.
- [4] Y. Giomataris *et al.*, Nucl. Instrum. Methods A **560** (2006) 405-408.
- [5] D. Thers *et al.* Nucl. Instrum. Methods A **469** (2001) 133146.
- [6] M. Bellis, V. Crede, S. Strauch (spokespersons), [http://www.jlab.org/exp\\_prog/proposals/06/PR06-013.pdf](http://www.jlab.org/exp_prog/proposals/06/PR06-013.pdf).
- [7] G. Charles *et al.*, submitted to Nucl. Instrum. Methods.
- [8] S. Procureur *et al.*, submitted to Nucl. Instrum. Methods.
- [9] Geant4 - a simulation toolkit, Nucl. Instrum. Methods A **506** (2003) 250.